Investigation of Electronic and Optical Properties of AlAs/In_<0.43>Ga_<0.57>As/GaAs_<0.55>Sb_<0.45> Nanoscale Heterostructure

Vijay, Jayprakash
Department of Electronics and Communication Engineering, Swami Keshvanand Institute of Technology, Management & Gramothan

Rawal, Pallav
Department of Electronics and Communication Engineering, Swami Keshvanand Institute of Technology, Management & Gramothan

Rathi, Amit
Department of Electronics and Communication Engineering, Manipal University Jaipur

https://doi.org/10.5109/7236830

出版情報：Evergreen. 11 (3), pp.1777-1783, 2024-09. Interdisciplinary Graduate School of Engineering Sciences, Kyushu University, Japan
バージョン：

Investigation of Electronic and Optical Properties of $AlAs/In_{0.43}Ga_{0.57}As/GaAs_{0.55}Sb_{0.45}$ Nanoscale Heterostructure

Jayprakash Vijay[1,*], Pallav Rawal[1], Amit Rathi[2]
[1]Department of Electronics and Communication Engineering, Swami Keshvanand Institute of Technology, Management & Gramothan, Jaipur, 302017 (India)
[2]Department of Electronics and Communication Engineering, Manipal University Jaipur, India

*Author to whom correspondence should be addressed:
E-mail: jpvijay121@gmail.com

(Received March 6, 2024: Revised May 3, 2024: Accepted June 24, 2024).

Abstract: Heterostructures composed of compound semiconductors hold significant promise for advancing near-infrared applications due to their unique electronic and optical properties. In this study, we present the design and simulation of a novel heterostructure tailored specifically for NIR functionality. The nanoscale heterostructure is designed using the compound semiconductors $AlAs/In0_{.43}Ga_{0.57}As/GaAs_{0.55}Sb_{0.45}$ and simulated for the applications of optical sources in near-infrared region. Through k.p method, we thoroughly investigate the electronic band structure, carrier transport properties, and optical response of the heterostructure. We also investigate how size of the quantum well layer affect the heterostructure performance, offering insightful information for future customization and optimization. The entire structure has been modeled at room temperature 300 K.

Keywords: Dispersion; Energy Wavefunctions; Heterostructure; Semiconductors; Quantum well

1. Introduction

Semiconductor heterostructures made from compound semiconductors have garnered significant attention in the field of optoelectronics due to their unique properties and versatile applications. The integration of multiple compound semiconductor materials in heterostructures enables the realization of advanced functionalities like bandgap engineering, tunable optical properties, enhanced carrier transport, lattice matching, strain engineering and quantum confinement effects, etc[1)]. In particular applications, material selection is important in heterostructure since the material affects the emission wavelength. For example, photodynamic therapy (PDT) uses red lasers with a wavelength of 635 nm to treat superficial skin problems[2)]. Optical sources operating in the near-infrared (NIR) range are used in optical fibre communication[3,4)] and spectroscopy[5)]. Terahertz spectroscopy relies on far-infrared lasers[6)].

A comprehensive literature review on heterostructures and quantum well structures made of semiconductors for LED, laser, and photodiode applications reveals a plethora of research highlighting their significance in optoelectronic devices[7,8)]. Kim et al. investigated the impact of interface engineering on the performance of GaN-based heterostructures for LEDs[9)]. Through systematic characterization and optimization, they demonstrated significant enhancements in device efficiency, paving the way for more energy-efficient and brighter LED technologies. Li et al. focused on the design and optimization of quantum well structures in semiconductor lasers[10)]. By carefully tailoring the bandgap of the active region, they achieved precise control over emission wavelengths, leading to improved spectral purity and device reliability in laser applications. N. Kumari et al. presented MATLAB-Based Simulation Analysis of the Partial Shading on PV Array Configuration[11)]. Zhang et al. explored the utilization of III-nitride heterostructures in photodiodes, showcasing their potential for high-speed and high-sensitivity photodetection[12)]. Their research highlighted the importance of material quality and interface properties in achieving optimal device performance for various photonic applications. Wu et al. introduced perovskite-based heterostructures as promising candidates for optoelectronic applications[13)]. Synthesis of ZnO Thin Film by Electroplating presented and Effect of Zinc Concentration on the Structural and Optical Properties demonstrated[14,15)]. By integrating perovskite materials into semiconductor heterostructures, they demonstrated improved device performance and versatility, opening up new avenues for next-generation optoelectronic devices. Choi et al. investigated the integration of two-dimensional materials into semiconductor heterostructures for advanced optoelectronic functionalities[16)]. Their research demonstrated enhanced light-matter interactions and tunable optical properties, offering opportunities for developing novel devices with tailored functionalities. Zhao et al. explored the use of quantum dot heterostructures for efficient light emission in LEDs and lasers[17)]. Through precise control over quantum dot properties and device architecture, they achieved enhanced optical performance and stability, promising advancements in semiconductor optoelectronics. Chen et al. investigated strain engineering techniques in semiconductor heterostructures for controlling emission wavelengths in optoelectronic devices[18)]. Their research demonstrated the feasibility of tuning optical properties through strain manipulation, offering a versatile approach for device optimization. Researchers also presented the explores the synergistic potential of natural dyes for enhancing opto-electronic device efficiency, offering promising insights into sustainable energy solutions[19, 20, 21)]. Wang et al. proposed nanowire-based heterostructures as building blocks for integrated photonic circuits[22)]. By leveraging the unique properties of nanowires, such as high surface-to-volume ratio and compatibility with scalable fabrication techniques, some researchers demonstrated compact and efficient photonic devices for diverse applications[23,24,25)]. Li et al. investigated hybrid organic-inorganic heterostructures for enhanced optoelectronic device performance[26)]. By combining organic and inorganic materials, they achieved synergistic effects that resulted in improved device efficiency, stability, and flexibility, offering promising prospects for future optoelectronics. Wong et al. studied ultrafast carrier dynamics in semiconductor heterostructures for understanding and optimizing device performance[27)]. Their research provided insights into charge transport mechanisms and recombination dynamics, facilitating the design of ultrafast optoelectronic devices with superior performance. Wang et al. presented a comprehensive study on the epitaxial growth and characterization of GaAs/AlGaAs/InGaAs heterostructures for efficient light-emitting diodes (LEDs)[28)]. Their work demonstrates the synergistic effects of different semiconductor materials in enhancing device performance and provides valuable insights into the optimization of multilayer heterostructures for optoelectronics. Furthermore, advancements in fabrication techniques, such as molecular beam epitaxy (MBE) and metalorganic chemical vapor deposition (MOCVD), have played a pivotal role in achieving precise control over heterostructure properties[29,30,31)]. Liang et al. investigated the growth kinetics of InGaAs/InAlAs heterostructures using MBE, elucidating the influence of growth parameters on interface quality and material properties[32)]. Their findings contribute to the optimization of growth processes for high-quality heterostructure fabrication. These studies collectively underscore the continuous efforts in tailoring semiconductor heterostructures and quantum well architectures for next-generation optoelectronic devices paving the way for advancements in LED, laser, and photodiode technologies[33,34)]. The wavelength that heterostructure emits determines the type of application that they can be used for. This in turn depends on the material that was used to manufacture the heterostructure. As such, the choice of material is crucial to the design of heterostructures.

The objective of this work is to design a heterostructure for near-infrared (NIR) applications. The specific application depends on the emission wavelength, which is determined by the material's bandgap. Thus, selecting the appropriate material is crucial, as it dictates the emission wavelength. Ternary materials and heterostructure layer sizes were optimized to achieve the desired bandgap energy for NIR radiation emission. The selection process likely prioritized compound semiconductors with suitable bandgap energies, high carrier mobilities, lattice matching, optical transparency, heterostructure band offsets, and material stability to ensure optimal performance in NIR optoelectronic applications.

2. Design Specification and Simulation Outcome

To investigate energy wavefunctions, dispersion profiles, and optical gain, this research models a nanoscale heterostructure (QW structure) composed of $AlAs/In_{0.43}Ga_{0.57}As/GaAs_{0.55}Sb_{0.45}$ layers on a GaAs substrate at room temperature. Figure 1 illustrates the structure's energy band diagram. The $In_{0.43}Ga_{0.57}As$ quantum well layer has a width of 2 nm, the $GaAs_{0.55}Sb_{0.45}$ barrier layer is 4 nm thick, and the AlAs cladding layer is 10 nm thick. These dimensions were determined through multiple calculations to maximize charge carrier confinement and efficient recombination, enhancing optical gain at targeted NIR wavelengths. The size of the quantum well and other layers were optimized to fine-tune the bandgap energy, ensuring emission at the desired wavelength for optical fiber communication applications. This optimization process allows precise control over the bandgap energy and emission wavelength, with material properties and device performance considered to ensure optimal functionality and efficiency.

The heterostructure's layers of composite materials are only a few nanometer diameters, so charge carrier excitons are impacted and electrons can only occupy distinct levels of energy. For understanding the lasing behaviour of the proposed heterostructure necessitates a comprehension of bulk materials, which serve as the foundation for structural design. Employing the 8-band Hamiltonian model with effective mass approximation, the band structures of ternary compounds $In_{0.43}Ga_{0.57}As$ and $GaAs_{0.55}Sb_{0.45}$ on GaAs substrate have been determined[35)]. Figures 2 and 3 illustrate the band structure diagrams of bulk materials grown at room temperature (300 K) on the GaAs substrate, revealing three sub-bands in the valence band: the heavy hole subband (HH), light hole sub-band (LH), and split-off sub-band (SOB), classified based on hole effective masses. Notably, at zero momentum (Kz = 0), the heavy hole band is positioned above the light hole band in both bulk materials; however, this characteristic is altered due to internal strain within the materials grown on the GaAs substrate. Additionally, the split-off band exhibits lower energy and remains distant from the top of the valence band, thereby posing minimal concerns regarding the effective recombination of electrons from the conduction band and holes from the valence band. The performance and efficacy of the heterostructure presented in this work are influenced by several critical design parameters like Layer Composition and Thickness, Band Alignment and Band Offsets, Quantum Well Dimensions: Doping Profile: Temperature Stability, etc.

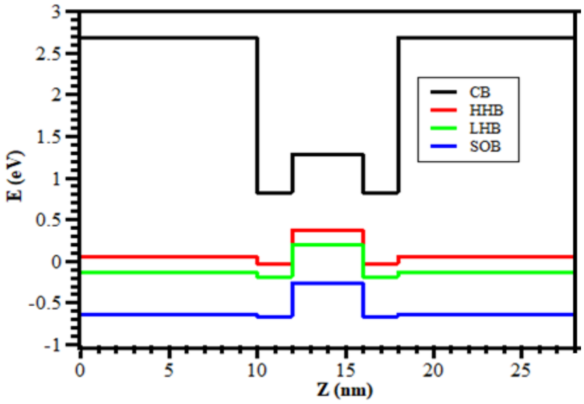

Fig. 1: Energy band diagram of designed $AlAs/In_{0.43}Ga_{0.57}As/GaAs_{0.55}Sb_{0.45}$ heterostructure

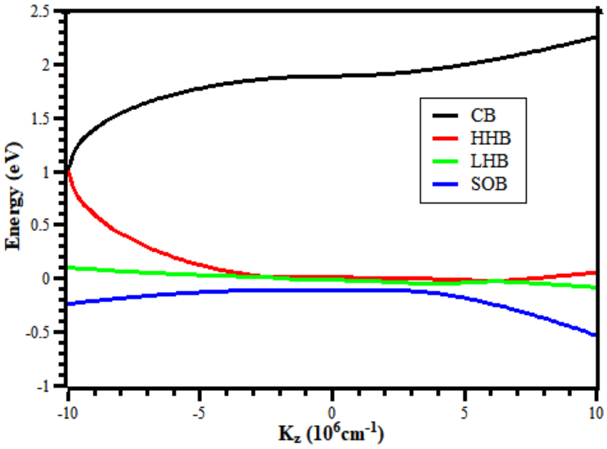

Fig. 2: The structural arrangements of ternary compound $In_{0.43}Ga_{0.57}As$

Once the band structure and energy band diagram of heterostructure has been acquired, it becomes feasible to customize its electronic and optical traits. The k.p. method, widely employed in the scientific community, facilitates the calculation of these properties by leveraging knowledge of wave functions and confinement states[36]. Perturbation theory, integral to the k.p technique, delineates energy levels in the E-k space near the k = 0 point. In this study, the targeted structures have been meticulously examined through the application of the 6-band k.p model. The computed energy wavefunctions for the designed heterostructure are shown in Fig. 4. It illustrates a notable confinement phenomenon: electrons exhibit high confinement within the quantum well of the $In_{0.43}Ga_{0.57}As$ as material, whereas holes experience pronounced confinement within the barrier material $GaAs_{0.55}Sb_{0.45}$. Consequently, the quantum well regions boast elevated total electron density, while the barrier region demonstrates heightened total hole density. In the envisaged type-II heterostructure, optical transitions are anticipated to occur from the electrons within the well regions to the holes within the barrier region.

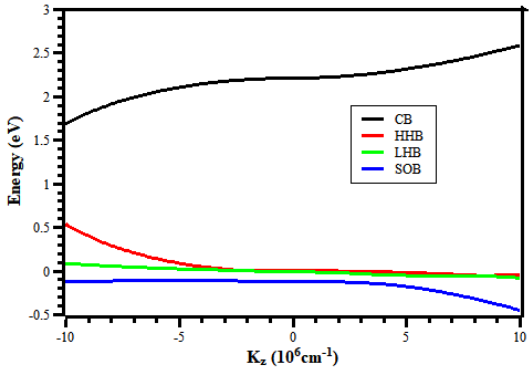

Fig. 3: The structural arrangements of ternary compound $GaAs_{0.55}Sb_{0.45}$

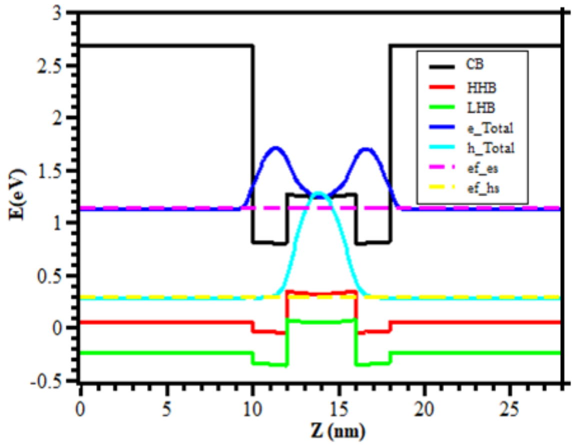

Fig. 4: Net wavefunctions of designed $AlAs/In_{0.43}Ga_{0.57}As/GaAs_{0.55}Sb_{0.45}$ heterostructure

Following the determination of carrier density in the designed nanoscale heterostructure, a dispersion curve is generated to depict the behavior of carriers within both conduction and valence bands. Figure 5 illustrates the dispersion profile of the $AlAs/In_{0.43}Ga_{0.57}As/GaAs_{0.55}Sb_{0.45}$ heterostructure, showcasing two energy levels for conduction band electrons (E1 and E2) and three energy levels for valence band holes (HH11, HH2, and HH3). Analysis of the dispersion curve reveals a nearly parabolic profile for the conduction band, indicating numerous allowed energy states, while the valence band exhibits a non-parabolic shape, with heavy holes playing a significant role in electronic transitions. At k=0, direct band gap alignment is evident, suggesting a higher recombination rate, meeting the criteria for achieving high optical gain and amplification.

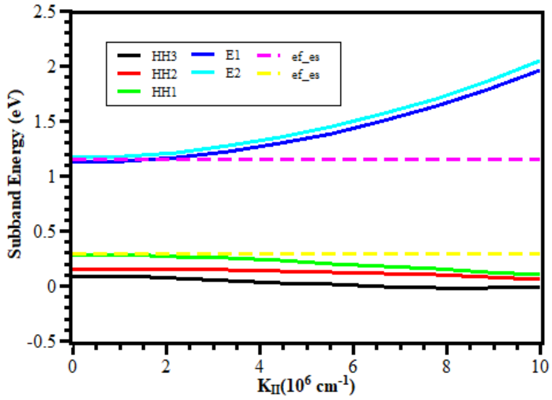

Fig. 5. Dispersion curve for designed $AlAs/In_{0.43}Ga_{0.57}As/GaAs_{0.55}Sb_{0.45}$ heterostructure

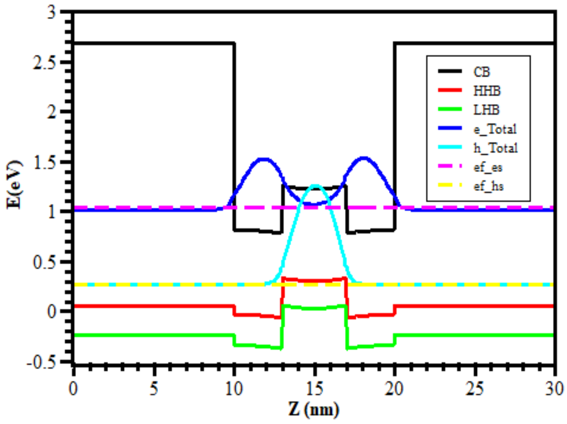

Fig. 6: Energy wavefunctions for $AlAs/In_{0.43}Ga_{0.57}As/GaAs_{0.55}Sb_{0.45}$ heterostructure for thicknesses of QW=3 nm

For all the above analyses, the size of the quantum well layer was 2 nm and the size of the barrier layer was 4 nm. The molar fractions and the materials are chosen based on their suitability for NIR emissions after multiple calculation. Moreover, the effects of the quantum well thickness is also studied in further work. Since the thickness of the well and the barrier affect the energy levels and modify the bandgap of the materials. Figures 6, 7 & 8 show the computed wavefunctions related to the holes of the valance band and electrons of the conduction band for the designed heterostructure with the quantum well thickness 3 nm, 4 nm and 5 nm respectively. In all these calculations, the thickness of the barrier layer is 4 nm and the thickness of the cladding layer is 10 nm. From this analysis, it is observed that as we increase the size of the quantum well layer the bandgap of the material shifts toward the higher side and the transition strength of the charge carrier decrease. The optical transition will occur between electrons of the quantum well and holes of the barrier, where the respective charge carrier density is larger. The electronic and optical properties of a quantum well in a heterostructure undergo substantial alterations as its size is modified. As the well size gets smaller, quantum confinement effects become more noticeable and separate electron and hole energy levels result. As a result of the higher bandgap energy, the emission wavelength changes. Furthermore, the density of states constricts, influencing the dynamics of recombination and carrier mobility. Additionally, variations in the size of the quantum well affect the electronic band structure, which modifies characteristics like effective mass and band alignment at interfaces and affects the functionality of the device in optoelectronic applications.

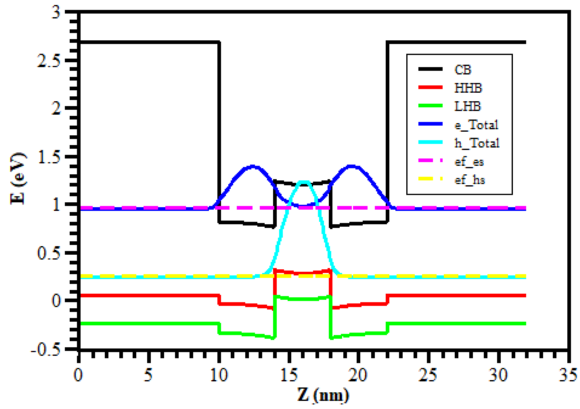

Fig. 7: Energy wavefunctions for $AlAs/In_{0.43}Ga_{0.57}As/GaAs_{0.55}Sb_{0.45}$ heterostructure for thicknesses of QW=4 nm

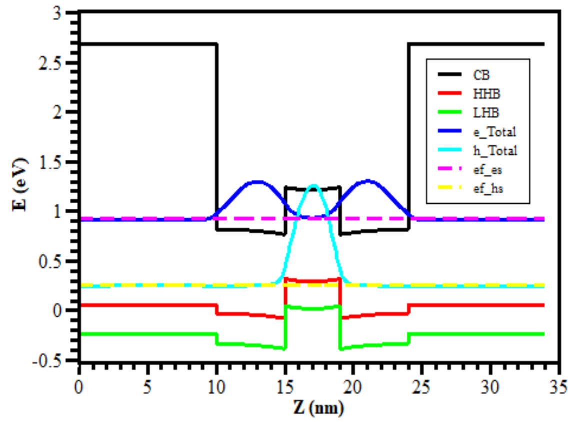

Fig. 8: Energy wavefunctions for AlAs/In0.43Ga0.57As/GaAs0.55Sb0.45 heterostructure for thicknesses of QW=5 nm

After the computation of the wavefunctions, the optical gain characteristics are computed for the quantum well thickness of 2 nm, 3 nm, 4 nm and 5 nm respectively. Figure 9 illustrates a comprehensive plot correlating the calculated optical gain per unit length (expressed in inverse centimeters) with both photonic energies, specifically observed at room temperature. From this, it is observed that as we increase the size of the QW layer the optical gain decreases due to a decrement in the density of the carrier. Table 1 presents the computed optical gain and emitted wavelengths for different thicknesses of the quantum well layer. An analysis of the optical gain characteristics reveals the heterostructure's remarkably narrow spectral width, highlighting its potential suitability for laser applications within the near-infrared (NIR) region.

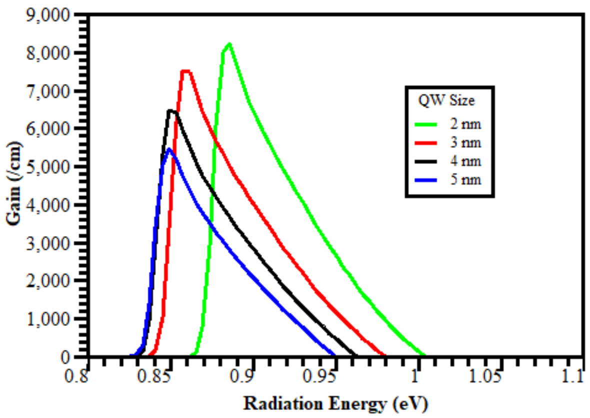

Fig. 9: Optical Gain characteristics of AlAs/In0.43Ga0.57As/GaAs0.55Sb0.45 heterostructure with variation in thickness of QW size

We believe that these theoretical insights and simulations presented in this paper lay a strong foundation for future experimental validation and fabrication efforts. However, MBE and MOVPE are precise deposition techniques can be used to grow crystalline layers of semiconductor materials with atomic-level control. MBE involves evaporating elemental sources in ultra-high vacuum conditions to create thin layers of materials on a substrate. MBE offers excellent control over layer thickness, composition, and interface quality, making it well-suited for fabricating heterostructures with precise layer arrangements. For reference, the table 2 illustrates various fabrication techniques utilized for structures of this type, indicating the feasibility of fabricating the designed heterostructure.

Table 1: Computation of optical gain and emission wavelength for $AlAs/In0._{43}Ga_{0.57}As/GaAs_{0.55}Sb_{0.45}$ heterostructure with different thickness of QW layer

QW Thickness	Optical gain (cm^{-1})	Emission energy (eV)	Emission wavelength (nm)
2 nm	8232	0.8858	1400
3 nm	7516	0.8575	1446
4 nm	6470	0.8494	1460
5 nm	5453	0.8454	1466

Table 2: Fabrication techniques utilized for related QW heterostructure

QW Structure	Fabrication technique	Emission wavelength (*nm*)	Ref
GaSb/AlGaSb	MBE	1650	37
GaInAs/GaAsSb	MOVPE	1200 to 1470	38
GaAsSb/lnGaAs	MBE	1380, 1430	39
GaAsSb/lnGaAs	MOVPE	1022, 1075	40
This work	6 band k p formalism (simulation)	1400	41

Future research could involve mathematical modeling, experimental validation of the heterostructure, and its integration into NIR optoelectronic devices like LEDs and photodetectors. Exploring alternative materials for bandgap tuning and studying temperature effects could further enhance applications in telecommunications, biomedical imaging, and environmental sensing, driving advancements in NIR technology.

3. Conclusion

Compound semiconductor heterostructures, including GaAs, AlGaAs, InGaAs, and InAlAs, hold immense potential for various optoelectronic applications. For the quantum well structure $AlAs/In_{0.43}Ga_{0.57}As/GaAs_{0.55}Sb_{0.45}$, the maximum optical gain is found of the order of 8232/cm at the photonic energy of 0.885 eV or 1400 nm quantum well thickness of 2 nm. Through adjustment of the quantum well's size in this heterostructure, we noted significant changes in optical gain and emission wavelength. The optical amplification capabilities of the heterostructure are directly affected by these modifications. Furthermore, our results highlight how crucial precise control over quantum well size is for creating optoelectronic devices with customized performance attributes. In addition to providing possible paths for enhancing the design and manufacture of next-generation photonic devices for a range of technological applications, this work makes a significant contribution to the field of semiconductor nanostructures.

References

1) U. Erkılıç, H. Ago, "Type-I Heterostructure and Improved Phase Stability of Formamidinium Lead Iodide Perovskite Grown on WS2", EVERGREEN Joint Journal of Novel Carbon Resource Sciences & Green Asia Strategy, 07 (3) 323-328 (2020). doi:10.5109/4068610
2) Peter M. Smewton, Gareth M.Lewis, Peter Blood, Weng W. Chow, "Optimization of 635-nm tensile strained GaInP Laser Diodes", IEEE Journal of Selected Topics In Quantum Electronics, Vol.- 9, no.-

5, pp.1246-1251, October 2003.
3) P. A. Alvi, Pyare Lal, S. Dalela, M. J. Siddiqui, "An Extensive Study on Simple and GRIN SCH based In0.71Ga0.21Al0.08As/InP Lasing heterostructure", Physica Scripta, 85, 035402, 2012.
4) S. Hein, A. Somers, S. Hofling, A. Forchel, "Low threshold high efficiency InAs/InGaAlAs/InP ~1.55 µm quantum dash-in-a-well lasers", IEEE 19th International Conference on Indium Phosphide & Related Materials, pp. 340-349, 2007.
5) Jan U. Porep, Dietmar R. Kammerer, Reinhold Carle, "On-line application of near infrared (NIR) spectroscopy in food production", Trends in Food Science & Technology, http://dx.doi.org/10.1016/j.tifs.2015.10.002, 2015.
6) Shriganesh S. Prabhu Terahertz Spectroscopy: Advances and Applications", Molecular and Laser Spectroscopy Advances and Applications, Pages 65-85, 2018.
7) Anthony Chukwunonso Opia, Mohd Kameil Abdul Hamid, Syahrullail, Samion, Charles A. N. Johnson, "Nano-Particles Additives as a Promising Trend in Tribology: A Review on their Fundamentals and Mechanisms on Friction and Wear Reduction.", EVERGREEN Joint Journal of Novel Carbon Resource Sciences & Green Asia Strategy, Evergreen, 8(4) 777-798 (2021). doi:10.5109/4742121
8) Nurdin Siregar, Motlan and Makmur Sirai, "Synthesis of ZnO Thin Film by Electroplating: Effect of Zinc Concentration on the Structural and Optical Properties", EVERGREEN Joint Journal of Novel Carbon Resource Sciences & Green Asia Strategy, 10(2) 715-721 (2023). doi:10.5109/6792820
9) J. Kim, J. Lee and G. Yang, "Interface-Engineered GaN-based Heterostructure for High-Performance Light-Emitting Diodes", Advanced Electronic Materials, 6(5) 190-201 (2020).
10) H. Li, D. Jiang, and Y. Wang, "Design and Optimization of Quantum Well Structures for Semiconductor Lasers", Journal of Semiconductors, 39(5) (2018).
11) N. Kumari, S. K. Singh, and S. Kumar, "MATLAB-Based Simulation Analysis of the Partial Shading at Different Locations on Series-Parallel PV Array Configuration", EVERGREEN Joint Journal of Novel Carbon Resource Sciences & Green Asia Strategy, 9(4) 1126-1139 (2022). doi:10.5109/6625724
12) L. Zhang, Y. Zhang, and J. Wang, "III-Nitride Heterostructures for High-Speed Photodetection", Journal of Physics D: Applied Physics, 52(24) (2019).
13) X. Wu, S. Yang, and Z. Xu, "Perovskite-Based Heterostructures for Optoelectronic Applications", Advanced Materials, 33(6) (2021).
14) N. Siregar, Motlan, and M. Sirait, "Synthesis of ZnO Thin Film by Electroplating: Effect of Zinc Concentration on the Structural and Optical Properties," EVERGREEN Joint Journal of Novel Carbon Resource Sciences & Green Asia Strategy, 10(2) 715-721 (2023). doi:10.5109/6792820
15) E.R. Dyartanti, I.N. Widiasa, A. Purwanto, and H. Susanto, "Nanocomposite polymer electrolytes in PVDF/ZnO membranes modified with PVP for use in LiFePO4 Batteries," Evergreen, 5 (2) 19–25 (2018). doi:10.5109/1936213.
16) S. Choi, J. Park, and S. Lee, "Two-Dimensional Materials for Optoelectronic Devices: Recent Advances and Perspectives", Nanotechnology, 30(50) (2019).
17) Y. Zhao, X. Wang, and Q. Li, "Quantum Dot Heterostructures for Efficient Light Emission: Progress, Challenges, and Opportunities", Advanced Optical Materials, 5(6) (2017).
18) Z. Chen, L. Wang, and W. Lu, "Strain Engineering in Semiconductor Heterostructures for Optoelectronic Applications", Advanced Functional Materials, 30(20) (2020).
19) Arifin, Zainal, Syamsul Hadi, Bayu Sutanto, and Denny Widhiyanuriyawan. "Investigation of Curcumin and Chlorophyll as Mixed Natural Dyes to Improve the Performance of Dye-Sensitized Solar Cells." Evergreen, 9 (1) 17–22 (2022) doi:10. 5109/4774212.
20) Y.D.Kim, K.Thu, K.Choon Ng, "Evaluation of parametric optimization of the thermal performance and cost-effectiveness of active-indirect solar hot water plants", Evergreen. Joint Journal of Novel Carbon Resource Sciences & Green Asia Strategy, 2(2), 50-60, (2015). doi:10.5109/1544080.
21) N. Kumari, S. Kumar Singh, S. Kumar, "Matlabbased simulation analysis of the partial shading at different locations on series-parallel PV array configuration", Evergreen. Joint Journal of Novel Carbon Resource Sciences & Green Asia Strategy, 9(4), 1126-1139, (2022). doi:10.5109/6625724
22) J. Wang, Y. Guo, and C. Ning, "Nanowire-Based Heterostructures for Integrated Photonic Circuits", Nano Letters, 18(9) 5741-5747 (2018).
23) Gupta, Gaurav, R. K. Tyagi, and S. K. Rajput. "A Statistical Analysis of Sputtering Parameters on Superconducting Properties of Niobium Thin Film." Evergreen, 8 (1) 44–50 (2021). doi:10.5109/4372259.
24) Ari Sulistyo Rini, Yolanda Rati, Raysa Fadillah, Rakhmawati Farma, Lazuardi Umar Yan Soerbakti, "Improved Photocatalytic Activity of ZnO Film Prepared via Green Synthesis Method Using Red Watermelon Rind Extract", VERGREEN Joint Journal of Novel Carbon Resource Sciences & Green Asia Strategy, Vol. 09, Issue 04, pp1046-1055, December 2022.
25) K. Taira, and H. Einaga, "Distribution ratio of Pt on anatase and rutile TiO2 particles, determined by X-ray diffraction and transmission electron miscroscopy

analysis of Pt/TiO2(P25),” Evergreen, 5 (4) 13–17 (2018). doi:10.5109/2174853.
26) T. Li, Y. Zhang, and S. Han, “Hybrid Organic-Inorganic Heterostructures for Enhanced Optoelectronic Device Performance”, Advanced Optical Materials, 9(14) (2021).
27) K. Wong, C. Chan, and K. Cheng, “Ultrafast Dynamics in Semiconductor Heterostructures for Optoelectronic Applications”, Advanced Science, 6(23) (2019).
28) H. Wang, "Efficient light-emitting diodes based on GaAs/AlGaAs/InGaAs heterostructures," Semiconductor Science and Technology, 38(5) (2023).
29) A.S. Idris, S. Ghosh, H. Jiang, and K. Hamamoto, “A multi-layer stacked all sol-gel fabrication technique for vertical coupled waveguide,” Evergreen, 4 (2/3) 12–17 (2017). doi:10.5109/1929657.
30) Y. Wu, B. Liu, F. Xu, Y. Sang, T. Tao, Z. Xie, K. Wang, X. Xiu, P. Chen, D. Chen, H. Lu, R. Zhang, and Y. Zheng, "High-efficiency green micro-LEDs with GaN tunnel junctions grown hybrid by PA-MBE and MOCVD," Photon. Res. 9, 1683-1688, 2021.
31) Jiadong Yu, Zhibiao Hao, Jian Wang, Jun Deng, Wangyang Yu, Lai Wang, Yi Luo, Yanjun Han, Changzheng Sun, Bing Xiong, Hongtao Li, "Study on AlN buffer layer for GaN on graphene/copper sheet grown by MBE at low growth temperature, Journal of Alloys and Compounds, Volume 783, Pages 633-642, ISSN 0925-8388, https://doi.org/10.1016/j.jallcom.2019.01.007, 2019.
32) Z. Liang, "Growth kinetics of InGaAs/InAlAs heterostructures by molecular beam epitaxy," Journal of Crystal Growth, 55(4) (2024).
33) X. Jiang, "Precise control of GaAs/AlGaAs heterostructures for optoelectronic applications," Applied Physics Letters, 123(15) (2023).
34) J. R. Smith, "Tuning optical properties of AlGaAs-based heterostructures through alloy composition," Journal of Applied Physics, 131(8) (2022)
35) I.Vurgaftman, J. R. Meyer and L.R. Ram-Mohan, “Band parameters for III–V compound semiconductors and their alloys”, Journal of Applied Physics, Vol. - 89, No.-11, PP. 5815-5863, June 2001.
36) J. M. Luttinger and W. Kohn, “Motion of Electrons and Holes in Perturbed Periodic Fields,” Phys. Rev. 97, p. 869, 1955.
37) M. Mehta et al., “Room-temperature operation of buffer-free GaSb–AlGaSb quantum-well diode lasers grown on a GaAs platform emitting at 1.65 μm,” IEEE Photonics Technol. Lett. 19(20), 1628–1630 (2007).
38) C. Fuchs et al., “Electrical injection type-II (GaIn) As/Ga (AsSb)/(GaIn) As single ‘W’-quantum well laser at 1.2 μm,” Electron. Lett. 52(22), 1875–1877 (2016).
39) C. Fuchs et al., “MOVPE growth of (GaIn) As/Ga (AsSb)/(GaIn) As type-II heterostructures on GaAs substrate for near infrared laser applications,” J. Cryst. Growth 464, 201–205 (2017).
40) J. F. Klein et al., “GaAsSb/InGaAs type-II quantum wells for long-wavelength lasers on GaAs substrates,” J. Vac. Sci. Technol. B 18(3), 1605–1608 (2000)